Published in final edited form as:
Cancer Prev Res (Phila). 2012 June ; 5(6): 810–821. doi:10.1158/1940-6207.CAPR-11-0532-T.

The CDK4/6 inhibitor PD0332991 reverses epithelial dysplasia associated with abnormal activation of the Cyclin-CDK-Rb pathway

M. Carla Cabrera[1], **Edgar S. Díaz-Cruz**[1,5], **Bhaskar V. S. Kallakury**[3,4], **Michael J. Pishvaian**[1,2,4], **Clinton J. Grubbs**[6], **Donald D. Muccio**[7], and **Priscilla A. Furth**[1,2,8]

[1]Department of Oncology, Georgetown University, Washington, DC, USA

[2]Department of Medicine, Georgetown University, Washington, DC, USA

[3]Department of Pathology, Georgetown University, Washington, DC, USA

[4]Lombardi Comprehensive Cancer Center, Georgetown University, Washington, DC, USA

[5]Department of Pharmaceutical Sciences, School of Pharmacy, Belmont University, Nashville, Tennessee, USA

[6]Departments of Surgery, Genetics, Medicine, University of Alabama at Birmingham, Birmingham, AL, USA

[7]Department of Chemistry, University of Alabama at Birmingham, Birmingham, AL, USA

[8]Department of Nanobiomedical Science and WCU Research Center of Nanobiomedical Science, Dankook University, Chungnam 330-714, Korea

Abstract

Loss of normal growth control is a hallmark of cancer progression. Therefore, understanding the early mechanisms of normal growth regulation and the changes that occur during preneoplasia may provide insights of both diagnostic and therapeutic importance. Models of dysplasia that help elucidate the mechanisms responsible for disease progression are useful in highlighting potential targets for prevention. An important strategy in cancer prevention treatment programs is to reduce hyperplasia and dysplasia. This study identified abnormal up-regulation of cell cycle related proteins Cyclin D1, CDK4, CDK6 and phosphorylated pRb as mechanisms responsible for maintenance of hyperplasia and dysplasia following down-regulation of the initiating viral oncoprotein Simian Virus 40 T Antigen. Significantly, p53 was not required for successful reversal of hyperplasia and dysplasia. Ligand-induced activation of RXR and PPAR gamma agonists attenuated Cyclin D1 and CDK6 but not CDK4 or phosphorylated pRb upregulation with limited reversal of hyperplasia and dysplasia. PD0332991, an orally available CDK4/6 inhibitor, was able to prevent upregulation of Cyclin D1 and CDK6 as well as CDK4 and phosphorylated pRb and this correlated with a more profound reversal of hyperplasia and dysplasia. In summary, the study distinguished CDK4 and phosphorylated pRb as targets for chemoprevention regimens targeting reversal of hyperplasia and dysplasia.

Keywords

dysplasia; chemoprevention; RXR/PPARgamma; PD0332991; CDK4/6

Corresponding author's contact information: Priscilla A. Furth, 3970 Reservoir Rd NW, Research Bldg. Room 520A, Georgetown University, Washington, DC, USA 20057, T: 202 687 8786; F: 202 687 7505, paf3@georgetown.edu.

INTRODUCTION

Although human dysplasia is considered to be a potentially reversible lesion, it has been difficult to develop appropriate therapies for this early pre-cancerous stage. Because genetically engineered *tetracycline-operator (tet-op)- Simian Virus 40 large T Antigen (TAg)*$^{Mouse\ Mammary\ Tumor\ Virus\ (MMTV)\text{-}\ tetracycline}$ TransActivator (tTA)) conditional mice demonstrate distinct phenotypes at 4- and 7-months of age following TAg down-regulation, they can be used to investigate molecular mechanisms responsible for the marked reversal of hyperplasia and dysplasia found at 4 months of age as compared to the 7-month-old mice that exhibit refractory hyperplasia and dysplasia (1–3). As previously published, when TAg is downregulated after 4 months, hyperplasia and dysplasia reverse through a re-differentiation process (2). However, when TAg is downregulated after 7 months, hyperplasia and dysplasia persist (1; 2). If TAg is not downregulated in this model, hyperplasia and dysplasia progress to invasive ductal adenocarcinoma and lung metastases (3) that, like the hyperplasia and dysplasia found at 7-months-of age, persist following down-regulation of TAg.

Interrupting cancer development by inducing resolution of precancerous lesions is an established cancer prevention goal (4). Mouse models are a tool for investigating the molecular mechanisms of persistent dysplasia and testing candidate chemopreventives (5; 6). This study was initiated to elucidate the molecular mechanisms responsible for maintaining the irreversible stage of epithelial cell dysplasia and to test candidate pharmacological agents UAB30, rosiglitazone, and PD0332991 for their ability to reverse this dysplasia.

Deregulation of the cell cycle machinery is a fundamental hallmark of cancer progression and a common feature in carcinogenesis (7). Here, we focused on understanding why cell proliferation would persist when, theoretically, loss of TAg should restore function of retinoblastoma protein (pRb) and associated family members (8). pRb is one of the major regulators of proliferation and its phosphorylation is governed by the cell cycle machinery (9). This machinery is made up of D and E-type cyclins, together with their associated kinases, CDK4, CDK6 and CDK2 (10). In early and mid-G1, D-type cyclins and their CDK4/6 kinase cohorts are responsible for initiating pRb phosphorylation, leading to its functionally inactive hyperphosphorylated state and consequent passage through the restriction point into S phase (9–11). Cancer progression studies have identified the importance of genes controlling G1 to S phase progression in the cell cycle including, CDK4, CDK6, Cyclin D1, its inhibitor p16, pRb, and p53 (7; 12; 13). Deregulation of p16, CDK4, CDK6 and Cyclin D activities have been implicated in different preneoplastic conditions (14; 15) and are targets for cancer chemoprevention (4). PD0332991 is a pyridopyrimidine-derived cyclin-dependent kinase (CDK) inhibitor with potential antineoplastic activity (16). Early reports documented its *in vitro* specificity against CDK4/6 and revealed its potent anti-proliferative activity against subcutaneous human tumor xenografts (16; 17). An important predictor of response to PD0332991 is the presence of pRb in the targeted cells (18). Here, we utilized PD0332991 to test if inhibition of the CDK4/6 pathway would promote regression of 'irreversible' dysplasia.

Like pRb, p53 activity also is restored when TAg is downregulated (8). Enhancing p53 activity is a one of the mechanisms hypothesized to be responsible for chemopreventive effects (19; 20). In this study, we utilized genetically modified mice with germ-line deficiency of p53 (*p53*$^{-/-}$) (21) to assess whether p53 was required for reversal of the dysplasia.

Rexinoid chemopreventives target the Retinoid X Receptor (RXR) (22) and may work, at least in part, by downregulating Cyclin D1 expression (23). Peroxisome proliferator-activated receptor gamma (PPARγ) forms heterodimers with RXR after activation (24), and combination treatment targeting both RXR and PPARγ has been reported to be more effective than single agent therapy (25). PPARγ agonists have also been shown to downregulate Cyclin D1 expression (26). We tested if the RXR agonist UAB30 (27) alone or in combination with PPARγ agonist rosiglitazone could promote regression of the 'irreversible' hyperplasia.

Results showed that the CDK4/6 inhibitor (PD0332991) was able to reverse previously 'irreversible' epithelial dysplasia associated with downregulation of CDK4, CDK6 and profound loss of pRb phosphorylation. In contrast, while the RXR and PPARγ ligands reduced levels of CDK6 and phosphorylated pRb, there was no significant impact on CDK4 expression levels and dysplasia was not reversed. p53 was found to be dispensable for the reversal process. The study points to a role for CDK4/6 inhibitors in chemoprevention.

MATERIALS AND METHODS

Mouse models and pharmaceutical agents

Tet-op-TAg$^{MMTV\text{-}tTA}$ and *tet-op-TAg*$^{MMTV\text{-}tTA/p53^{-/-}}$ mice were identified by polymerase chain reaction (PCR) (Transnetyx, Cordova, TN). *Tet-op-TAg*$^{MMTV\text{-}tTA/p53^{-/-}}$ mice were generated by breeding *Tet-op-TAg*$^{MMTV\text{-}tTA}$ mice (1) with p53+/− mice (21). Male mice were used to control for sexual dimorphic effects in salivary gland development (28). Cohorts of 7-month-old mice were randomized by dividing littermates into intervention or control groups. Submandibular salivary gland tissue was harvested during necropsy and snap frozen or fixed in 10% buffered formalin. Doxycycline was administered to downregulate TAg expression either in chow (200 mg/kg, Bio-Serv, Frenchtown, NJ) or in water (200 μg/ml, Fisher Scientific, Pittsburgh, PA) (2) either alone or concurrently with the following drugs: UAB30 (300 mg/kg/chow) alone or with rosiglitazone (400mg/kg/chow) for 14 or 28 days (provided by University of Alabama), or PD0332991 (150 mg/kg/oral gavage) (Selleck Chem, Houston, TX) for 10 days (prepared in 50 mM lactate buffer adjusted to pH 4) (18). To test if pharmaceuticals achieved targeted biological effects, TAg expression was assessed on western blots (doxycycline), liver retinyl palmitate was quantified by High Performance Liquid Chromatography (HPLC) (UAB30), and salivary gland expression levels of *adipose differentiation related protein (Adrp), fatty acid binding protein 4 (Fabp4), pyruvate dehydrogenase kinase isozyme 4 (Pdk4)* were measured by real-time reverse transcriptase PCR (RT-PCR) (UAB30, rosiglitazone). All procedures were performed in accordance with current Federal (NIH Guide for the Care and Use of Laboratory Animals) guidelines and approved by the Georgetown University Institutional Animal Use and Care Committee.

Histological analyses

For statistical analyses the extent of dysplasia was quantified by determining the percentage of hyperplastic and dysplastic, in-transition, and normal-like ductal structures (n=1000± 200 ductal structures counted/section) on hematoxylin and eosin (H&E)- stained formalin-fixed sections of the submandibular salivary gland. Normal-like structures were defined as fully striated differentiated ductal epithelial cells with monomorphic small nuclei. In-transition structures demonstrated partially striated ductal epithelial cells. Dysplastic structures were defined as ductal structures that did not contain any differentiated striated ductal cells. Hyperplastic structures were defined as structures with an abnormal increase in the number of ductal cells. An academic board certified pathologist (B.V.S.K.) blinded to the identity of the specimens and interventions identified normal-like, in-transition, hyperplastic and

dysplastic structures in the tissue sections. This analysis confirmed the significant differences in distribution of the four different types of structures in the different treatment and intervention groups.

Real-time RT-PCR

Total RNA was isolated using TRIzol (Invitrogen Life Technologies, Carlsbad, CA) (29). TaqMan Gene Expression Assays (ABI Prism 7700) detected *Adrp<* (*Pin1*) (Mm00475794_m1), *Fabp4* (Mm00445878_m1), *Pdk4* (Mm01166879_m1), *cyclin-dependent kinase 1 (Cdk1)* (Mm00772472_m1), *cell division cycle 25 homolog A (S. pombe) (Cdc25a)* (Mm00483162_m1), *retinoblastoma-like 1 (p107) (Rbl1)* (Mm01250721_m1), and 18s rRNA (Hs99999901_s1). Reactions were performed following manufacturer's recommendations using ABI Prism 7700 sequence detector and data analyzed with ABI Software (Applied Biosystems, Carlsbad, CA). Relative mRNA gene expression normalized against untreated control mice [$2-\Delta\Delta(Ct)$]; where $\Delta(Ct)$ = Ct (target gene) − Ct (18s rRNA) (30).

Western blots and immunohistochemistry

For western blots (WB), protein samples were quantified (29) and 60μg fractionated on 4–12% gradient Bis-Tris gels (NP0335; Invitrogen Life Technologies, Inc.), electrophoretically transferred onto nitrocellulose membranes (Amersham Biosciences, Piscataway, NJ), blocked in 5% nonfat dry milk in Tris-buffered saline and 0.1% Tween (one hour, room temperature) and exposed to the respective primary antibody overnight at 4°C. Membranes were exposed to the manufacturer-recommended dilution of the appropriate secondary antibody anti-rabbit NA934V (GE Healthcare, Piscataway, NJ), anti-goat SC-2768 or anti-mouse SC-2005 (Santa Cruz Biotechnology, Santa Cruz, CA). Proteins were visualized (ECL Plus Western Blotting Detection kit, Amersham Biosciences), quantified (Adobe Photoshop CS5, San Jose, CA) and mean relative densities and standard error of the mean (SEM) calculated after normalization to β-actin. Immunohistochemistry (IHC) was performed using Vectastain ABC or Mouse On Mouse (M.O.M) Peroxidase kits (Vector Laboratories, Inc., Burlingame, CA) following manufacturer's recommendations and digital photographs taken (Nikon Eclipse E800M microscope with DMX1200 software, Nikon Instruments, Inc., Melville, NY). WB primary antibodies: Anti-Cyclin D1 (DCS6) 1:2000, anti-CDK4 (DCS156) 1:1000, anti-CDK6 (DCS83) 1:1000, anti-Cyclin E (HE12) 1:1000, anti-pRb-Ser-807/811 (9308) 1:1000 (Cell Signaling Technology, Beverly, MA), Anti-CDK2 (sc-163) 1:200, anti-pRb (sc-50) 1:200, anti-p21 (sc-6246) 1:200, anti-p27 (sc-528) 1:200, anti-DP-1 (sc-610) 1:200, anti-E2F-1 (sc-193) 1:200, anti-TAg (sc-147) 1:200 (Santa Cruz Biotechnology Inc.). IHC primary antibodies: Anti-Cyclin D1 (sc-718) 1:50, anti-CDK6 (sc-7961) 1:50, anti-CDK4 (sc-260) 1:200, anti-CDK2 (sc-163) 1:1500, anti-Cyclin E (sc-198) 1:80, anti-p21 (sc-6246) 1:50, anti-pRb (sc-50) 1:25, anti-DP-1 (sc-610) 1:80, anti-E2F-1 (sc-193) 1:40 (Santa Cruz Biotechnology Inc.). Anti-pRb-Ser-807/811 (9308) 1: 100 (Cell Signaling Technology). Anti-p27 (610241) 1:3000 (BD Biosciences, Franklin Lakes, NJ).

Statistical analyses

Differences in relative protein expression levels and percentages of hyperplastic and dysplastic, in transition and normal-like ductal structures were compared using Student's *t* tests (two-tailed) and differences in relative RNA expression levels were compared using Mann Whitney *U* and one-way analysis of variance (ANOVA) (GraphPad Prism version 4.03 for Windows, GraphPad Software, San Diego, CA). Significance was assigned at $p \leq 0.05$.

RESULTS

Normal histology progressively established following TAg downregulation at 4- but not 7-months of age

TAg expression targeted to the submandibular salivary gland resulted in salivary dysplasia extending throughout most the gland by 4 months of age in *tet-op-TAg*$^{MMTV\text{-}tTA}$ mice (Fig. 1A). TAg downregulation led to reversal of hyperplasia and dysplasia and establishment of normal-like histology in 4- but not 7-month-old mice (Fig. 1A–H). The histological phenotype at both ages consisted of hyperplastic and/or dysplastic (Fig. 1A–C), in transition (Fig. 1D), or normal-like ductal structures (Fig. 1E) that resembled those of wild-type mice (Fig. 1F). While the percentages of these structures were similar at 4 and 7 months of age before TAg downregulation, the percentages were significantly different after TAg downregulation .The percentages of hyperplastic or dysplastic (*58% vs. 8%, $p<0.05$, Student *t* test (two-tailed) and in transition structures (**32% vs. 15%, $p<0.05$, Student *t* test (two sided) were significantly higher and the percentage of normal-like structures (***10% vs. 76%, $p<0.05$, Student *t* test (two-tailed) were significantly lower in 7- as compared to 4-month-old mice 14 days after TAg downregulation (Fig. 1G,H).

Activation of the Cyclin-CDK-Rb pathway following TAg downregulation correlated with maintenance of dysplasia

Expression levels of Cyclin D1, CDK6 and CDK4 were significantly higher in 7- as compared to 4-month-old mice 10 days after TAg downregulation (all $p<0.05$, Student *t* test (two-tailed). Expression levels of these proteins initially rose at both ages, but in 7-month-old mice they further increased while they fell to starting levels in 4-month-old mice (Fig. 2A–C). Phosphorylated pRb, DP-1 and E2F-1 were also expressed at significantly higher levels in the 7-month-old mice by the 14-day timepoint (all $p<0.05$, Student *t* test (two-tailed) (Fig. 2A,B,D,E). There was no significant increase in p21 and p27 expression in the 7-month-old mice, unlike the 4-month-old mice (Fig. 2A,B,F). Expression patterns of Cyclin E and CDK2 were similar in the 4- and 7-month-old mice with significantly higher levels of Cyclin E at the 10- and CDK2 at the 14-day timepoint in the 7-month-old mice (both $p<0.05$, Student *t* test (two-tailed) (Fig. 2A,B,G). Immunohistochemistry revealed parallel expression changes (Fig. 3A–K). Fourteen days after TAg downregulation 7-month-old mice showed increased expression of Cyclin D1, CDK6, CDK4, CDK2, phosphorylated pRb, DP-1 and E2F-1 with decreased expression of p21 and p27 as compared to 4-month-old mice. Real-time RT-PCR was used to evaluate whether or not these changes in cell cycle regulatory gene expression altered RNA expression levels of known E2F target genes *Cdk1, Rbl1, and Cdc25a* in the submandibular salivary tissue (Supp. Fig. 1). Whereas prior to TAg downregulation expression levels were equivalent in 4- and 7-month-old mice, after 14 days of doxycycline expression levels of *Cdk1* and *Rbl1* were significantly higher in the 7-month-old mice (both $p<0.05$, ANOVA). This was due to the more modest reduction in *Cdk1* and *Rbl1* gene expression seen in the 7- as compared to 4-month old mice following TAg downregulation. In contrast, *Cdc25a* expression was equivalently reduced in 4- and 7-month-old mice following TAg downregulation ($p<0.05$, ANOVA).

p53 was not required for dysplasia reversal following TAg downregulation in 4-month-old mice

p53 is one regulator of p21 and p27 expression. Theoretically, downregulation of TAg expression would restore p53 function and increase p21 and p27 expression (8,19,20). To test if p53 and associated p21 and p27 upregulation were required for dysplasia reversal, the extent of hyperplasia and dysplasia as well as gene expression changes were compared before and after TAg downregulation in 4-month-old *tet-op-TAg*$^{MMTV\text{-}tTA/p53^{-/-}}$ mice. The percentage of hyperplastic and dysplastic structures was significantly lower 14 days after

TAg downregulation (28% vs. 5%, p<0.01, Student *t* test (two-tailed) even though p53 was absent and there was no upregulation of p21 or p27 (Fig. 4A). Expression levels of cyclin D1, CDK6, CDK4, CDK2, phosphorylated pRb, DP-1 and E2F-1 at the 14-day timepoint were not significantly different compared to 4-month-old *tet-op-TAg*$^{MMTV\text{-}tTA}$ but were significantly lower when compared to 7-month-old *tet-op-TAg*$^{MMTV\text{-}tTA}$ mice (all p<0.05, Student *t* test (two-tailed) (Fig. 4B). A provocative finding was the significantly lower extent of dysplasia at baseline in mice lacking p53 as compared to mice with intact p53 (28% vs. 90%, p ≤0.0079, Student *t* test (two-tailed) (Figs. 1G, 4A).

Treatment with RXR and PPARγ agonists UAB30 and rosiglitazone downregulated expression levels of Cyclin D1, CDK6, phosphorylated Rb and E2F1 but did not change percentage of normal-like structures found in 7-month-old mice following TAg downregulation

To test if UAB30 or the combination of UAB30 with rosiglitazone could promote restoration of normal-like structures in the submandibular salivary tissue or impact expression of cell cycle regulatory genes in 7-month-old mice following TAg downregulation, UAB30 was administered for either 14 or 28 days alone or in combination with rosiglitazone (ROSI) for 28 days. No significant change in the percentage of differentiated normal-like ductal structures were found in the treated mice as compared to untreated controls at the same timepoint following TAg downregulation (Fig. 5A,B, data not shown for UAB30 treatment alone for 28 days). However, Cyclin D1, CDK6, phosphorylated pRb and E2F-1 were significantly lower in mice exposed to UAB30 and rosiglitazone for 28 days (all p<0.05, Student *t* test (two-tailed) (Fig. 5C,D). In contrast, expression levels of CDK4 and DP-1 were not significantly changed (Fig. 5C,D). Expression levels of E2F downstream genes *Cdk1* and *Rbl1* were reduced but remained significantly higher than those measured in 4-month old mice treated with doxycycline for 14 days (p<0.05, ANOVA) (Supp. Fig 1). Downregulation of TAg was confirmed by western blot (Suppl. Fig. 2A). To test if drug levels delivered were sufficient to impact expression levels of RXR and PPARγ downstream genes in the submandibular salivary gland and/or reduce liver retinyl palmitate protein levels (31), steady state RNA expression levels of *Fabp4*, *Adrp* and *Pdk4* in salivary and protein levels of retinyl palmitate in liver tissue were compared to untreated controls in all three treatment groups. Expression levels of all three genes were significantly increased by 14 days of UAB30 treatment with no further increase by extension of UAB30 treatment to 28 days or addition of rosiglitazone in a 28 day regimen (all p<0.05 compared to no treatment, Mann Whitney *U* test) (Fig. 5E). In contrast, liver retinyl palmitate levels were not significantly reduced after 14 days of UAB30 treatment but were significantly reduced after 28 days of treatment with UAB30 alone and UAB30+ROSI (both p<0.02, Student's *t* test, two-tailed) (Suppl. Fig. 3).. These results indicated that drug levels achieved by 28 days of UAB30 and rosiglitazone treatment were sufficient to impact gene expression in the salivary gland as well as alter liver metabolism. A comparison of the expression patterns of cell cycle regulatory proteins accompanying reversal to normal-like ductal structures in 4-month-old mice to the pattern following treatment with UAB30 and ROSI suggested that significant downregulation of CDK4 and/or DP-1 could be required, perhaps in addition to the changes in other cell cycle regulatory proteins, to promote the appearance of normal-like ductal structures.

The CDK4/6 inhibitor PD0332991 reversed the 'irreversible' dysplasia in 7-month-old mice

CDK4 and DP-1 were identified as potential key targets for downregulation in experiments presented above suggesting that a CDK4/6 inhibitor might be successful in promoting regression of refractory dysplasia. Ten days of exposure to the CDK4/6 inhibitor PD0332991 significantly reduced the percentage of hyperplastic and dysplastic ductal structures (*58% vs. 7%, p<0.01, Student *t* test (two-tailed) and significantly increased the

percentage of normal-like structures (**9% vs. 62%, p<0.01, Student *t* test (two-tailed) as compared to untreated controls at the same timepoint following TAg downregulation (Fig. 6A). Cyclin D1, CDK6, CDK4, phosphorylated pRb, DP-1 and E2F-1 were significantly reduced and p21 and p27 significantly increased as compared to untreated controls (all p<0.05, Student *t* test (two-tailed) (Fig. 6B,C). Parallel changes were found by immunohistochemistry (Fig. 6D). Expression levels of E2F downstream genes *Cdk1* and *Rbl1* were not significantly different than those quantified in 4-month-old mice treated with 14 days of doxycycline (Suppl. Fig.1) illustrating that all the molecular changes measured in the 4-month-old mice receiving doxycycline alone were paralled in the 7-month-old mice that received PD0332991 with doxycycline. Downregulation of TAg was confirmed by western blot (Suppl. Fig.2B).

DISCUSSION

Maintenance of cell cycle checkpoints is an obligatory element of normal cells to avert malignant transformation through uncontrolled growth. Here, we demonstrate that the Cyclin-CDK-Rb pathway can be activated in response to oncoprotein downregulation in a time-dependent ‘hit-and-run’-type model and that this activation is sufficient to maintain dysplasia. Perhaps more importantly, our experiments demonstrated that an orally available CDK4/6 inhibitor was able to reverse this dysplasia. Such drugs may be well-tolerated as many physiologically mediated growth signals still elicit normal responses even when levels of cell cycle effector proteins are low (32–35). It is possible that a requirement for upregulated Cyclin-CDK-Rb pathway may be limited to cells responding to mitogenic signals leading to malignant transformation (33) and targeting of these cell cycle proteins might resolve dysplasia while leaving normal cells unaffected (36–38).

The majority of established cancer therapies are cytotoxic agents designed to kill cells (39). In the last decade, cytostatic drugs that inhibit tumor growth in part by decreasing cell proliferation without direct cell killing were developed for their lower toxicity and increased tolerance (40). However, in cancers, single agent cytostatic drugs have not been as efficacious as required leading to the use of combination therapies with both cytotoxic and cytostatic agents (40). Chemoprevention aims to reverse or halt the progression of neoplastic cells to invasive malignancies and cytostatic agents that do so without direct killing have been proposed as potential therapies (20; 41; 42). In this study, a single cytostatic agent, PD0332991, which specifically targets CDK4/6, was sufficient to reverse refractory dysplasia.

Both biologically-mediated dysplasia reversal in 4-month-old mice and pharmacological reversal in 7-month-old-mice 14 and 10 days following TAg downregulation were associated with an increased percentage of normal-like structures that was correlated with multi-fold reductions in levels of CDK6, CDK4 and phosphorylated pRb (4- and 4-fold for CDK6, 22- and 11- fold for CDK4 and 68- and17-fold for phosphorylated pRb, respectively) and significant reductions in E2F target genes *Cdk1* and *Rbl1*. In contrast, no increased percentage of normal-like structures was found with the more modest 3-fold changes in CDK6 and phosphorylated pRb levels and unchanged CDK4 levels following up to 28 days of treatment with UAB30 and rosiglitazone and expression levels of *Cdk1* and *Rbl1* were not reduced to the same extent as found following PD0332991 treatment. This suggests that there are thresholds of changes in cell cycle regulators that are necessary to meet in order to restore normal-like tissue histology. These parameters of change may serve as molecular measures of therapeutic efficacy in trials of candidate chemopreventive regimens. .

SV40 large T antigen (TAg) is a potent oncoprotein that has been shown to transform a variety of cell types. The transformation potential of TAg is largely attributed to its

disruption of the p53 and pRb tumor suppressor proteins (43; 44). TAg can bind directly to the specific DNA binding domain of p53, and it has been hypothesized that upon binding, TAg inactivates the tumor suppressor function of p53 (8). However, the binding of p53 with TAg also increases the half-life and steady-state levels of p53 in cell culture partly due to the entrapment of the p300/mdm2/p53 complex that targets p53 for degradation (45; 46). *In vitro* tissue culture cell studies have suggested an unexpected role for p53 within the TAg complex by showing that the TAg-p53 complex has growth stimulatory activities that are required for malignant cell growth (47). Depletion of p53 then leads to structural rearrangements of the multiprotein complex resulting in growth arrest (47). The experiments presented here suggest this may also occur *in vivo* in whole tissue because the salivary glands in our *tet-op-TAg*$^{MMTV\text{-}tTA/p53^{-/-}}$ mice exhibited less dysplasia than the aged-matched *tet-op-TAg*$^{MMTV\text{-}tTA}$ controls with intact p53. Significantly, the negative cell cycle regulators p53, p21 and p27 did not appear to play a significant role in dysplasia reversal underscoring the importance of the Cyclin-CDK-Rb pathway in maintenance of the dysplasia. Interestingly, the positive cell cycle regulator *Cdc25a* may also be disconnected from dysplasia reversal in this model as its expression was repressed with downregulation of TAg regardless of whether or not dysplasia reversal occurred. This direct correlation with TAg expression may be similar to that reported for human papillomavirus E6/E7 protein expression and *Cdc25a* (48). Like TAg, the papillomavirus E6/E7 proteins also target and inactivate Rb and p53.

Our studies showed that the Cyclin-CDK-Rb pathway was activated in a time-dependent manner following oncoprotein downregulation and served to maintain dysplasia in the absence of the initiating oncoprotein. The CDK4/6 specific inhibitor, PD0332991 was used to demonstrate that effective targeting of this pathway was associated with reversal of dysplasia and hyperplasia. It is possible that alternative RXR or PPARγ agonists or longer regimens not tested here could more effectively target this pathway as an alternative RXR agonist LG100268 was reported to reverse dysplasia in lung epithelium (49). Next steps for the experiments presented here would be to determine how durable the reversal response of a 10-day PD0332991 treatment course is by following mice after treatment and evaluating if dysplasia returns as well as directly comparing the cancer preventive efficacy of the different regimens investigated here.

In summary, our results indicate a candidate mechanism for reversal of hyperplasia and dysplasia and provide parameters to follow in evaluating potential biomarkers of response.

Supplementary Material

Refer to Web version on PubMed Central for supplementary material.

Acknowledgments

Project was supported by NIH NCI RO1 CA112176 (P.A.F.), NIH NCI 2RO1 CA88041-1OS1 (P.A.F.), WCU (World Class University) program through the National Research Foundation of Korea funded by the Ministry of Education, Science and Technology (R31-10069) (P.A.F.), The Susan B. Komen Breast Cancer Foundation KG080359 (P.A.F.), NIH IG20 RR025828-01 (Rodent Barrier Facility Equipment), and NIH NCI 5P30CA051008 (Histology and Tissue; Genomic and Epigenomics and Animal Shared Resources).

References

1. Ewald D, Li M, Efrat S, Auer G, Wall RJ, Furth PA, et al. Time-sensitive reversal of hyperplasia in transgenic mice expressing SV40 T antigen. Science. 1996; 273:1384–1386. [PubMed: 8703072]
2. Tilli MT, Hudgins SL, Frech MS, Halama ED, Renou J-P, Furth PA. Loss of protein phosphatase 2A expression correlates with phosphorylation of DP-1 and reversal of dysplasia through

differentiation in a conditional mouse model of cancer progression. Cancer Res. 2003; 63:7668–7673. [PubMed: 14633688]

3. Furth PA, Li M, Hennighausen L. Studying development of disease through temporally controlled gene expression in the salivary gland. Ann N Y Acad Sci. 1998; 842:181–187. [PubMed: 9599308]
4. Dragnev KH, Feng Q, Ma Y, Shah SJ, Black C, Memoli V, et al. Uncovering novel targets for cancer chemoprevention. Recent Results Cancer Res. 2007; 174:235–243. [PubMed: 17302201]
5. Cardiff RD, Anver MR, Boivin GP, Bosenberg MW, Maronpot RR, Molinolo AA, et al. Precancer in mice: animal models used to understand, prevent, and treat human precancers. Toxicol Pathol. 2006; 34:699–707. [PubMed: 17074738]
6. Hursting SD, Nunez NP, Patel AC, Perkins SN, Lubet RA, Barrett JC. The utility of genetically altered mouse models for nutrition and cancer chemoprevention research. Mutat Res. 2005; 576:80–92. [PubMed: 15990122]
7. Cordon-Cardo C. Mutations of cell cycle regulators. Biological and clinical implications for human neoplasia. Am J Pathol. 1995; 147:545–560. [PubMed: 7677168]
8. Ali SH, DeCaprio JA. Cellular transformation by SV40 large T antigen: interaction with host proteins. Semin Cancer Biol. 2001; 11:15–23. [PubMed: 11243895]
9. Yu B, Lane ME, Pestell RG, Albanese C, Wadler S. Downregulation of cyclin D1 alters cdk 4- and cdk 2-specific phosphorylation of retinoblastoma protein. Mol Cell Biol Res Commun. 2000; 3:352–359. [PubMed: 11032757]
10. Kastan MB, Bartek J. Cell-cycle checkpoints and cancer. Nature. 2004; 432:316–323. [PubMed: 15549093]
11. Hinds PW, Dowdy SF, Eaton EN, Arnold A, Weinberg RA. Function of a human cyclin gene as an oncogene. Proc Natl Acad Sci U S A. 1994; 91:709–713. [PubMed: 8290586]
12. Soni S, Kaur J, Kumar A, Chakravarti N, Mathur M, Bahadur S, et al. Alterations of rb pathway components are frequent events in patients with oral epithelial dysplasia and predict clinical outcome in patients with squamous cell carcinoma. Oncology. 2005; 68:314–325. [PubMed: 16020958]
13. Aaltonen K, Amini RM, Landberg G, Eerola H, Aittomaki K, Heikkila P, et al. Cyclin D1 expression is associated with poor prognostic features in estrogen receptor positive breast cancer. Breast Cancer Res Treat. 2009; 113:75–82. [PubMed: 18240019]
14. Said TK, Moraes RC, Singh U, Kittrell FS, Medina D. Cyclin-dependent kinase (cdk) inhibitors/cdk4/cdk2 complexes in early stages of mouse mammary preneoplasia. Cell Growth Differ. 2001; 12:285–295. [PubMed: 11432803]
15. Lonardo F, Rusch V, Langenfeld J, Dmitrovsky E, Klimstra DS. Overexpression of cyclins D1 and E is frequent in bronchial preneoplasia and precedes squamous cell carcinoma development. Cancer Res. 1999; 59:2470–2476. [PubMed: 10344760]
16. Toogood PL, Harvey PJ, Repine JT, Sheehan DJ, VanderWel SN, Zhou H, et al. Discovery of a potent and selective inhibitor of cyclin-dependent kinase 4/6. J Med Chem. 2005; 48:2388–2406. [PubMed: 15801831]
17. Fry DW, Harvey PJ, Keller PR, Elliott WL, Meade M, Trachet E, et al. Specific inhibition of cyclin-dependent kinase 4/6 by PD 0332991 and associated antitumor activity in human tumor xenografts. Mol Cancer Ther. 2004; 3:1427–1438. [PubMed: 15542782]
18. Michaud K, Solomon DA, Oermann E, Kim J-S, Zhong W-Z, Prados MD, et al. Pharmacologic inhibition of cyclin-dependent kinases 4 and 6 arrests the growth of glioblastoma multiforme intracranial xenografts. Cancer Res. 2010; 70:3228–3238. [PubMed: 20354191]
19. Shankar S, Suthakar G, Srivastava RK. Epigallocatechin-3-gallate inhibits cell cycle and induces apoptosis in pancreatic cancer. Front Biosci. 2007; 12:5039–5051. [PubMed: 17569628]
20. Na H-K, Surh Y-J. Modulation of Nrf2-mediated antioxidant and detoxifying enzyme induction by the green tea polyphenol EGCG. Food Chem Toxicol. 2008; 46:1271–1278. [PubMed: 18082923]
21. Donehower LA, Harvey M, Slagle BL, McArthur MJ, Montgomery CA, Butel JS, et al. Mice deficient for p53 are developmentally normal but susceptible to spontaneous tumours. Nature. 1992; 356:215–221. [PubMed: 1552940]
22. Tanaka T, De Luca LM. Therapeutic potential of “rexinoids“ in cancer prevention and treatment. Cancer Res. 2009; 69:4945–4947. [PubMed: 19509234]

23. Li Y, Shen Q, Kim H-T, Bissonnette RP, Lamph WW, Yan B, et al. The rexinoid bexarotene represses cyclin D1 transcription by inducing the DEC2 transcriptional repressor. Breast Cancer Res Treat. 2011; 128:667–677. [PubMed: 20821348]
24. Wang T, Xu J, Yu X, Yang R, Han ZC. Peroxisome proliferator-activated receptor gamma in malignant diseases. Crit Rev Oncol Hematol. 2006; 58:1–14. [PubMed: 16388966]
25. Mehta RG, Williamson E, Patel MK, Koeffler HP. A ligand of peroxisome proliferator-activated receptor gamma, retinoids, and prevention of preneoplastic mammary lesions. J Natl Cancer Inst. 2000; 92:418–423. [PubMed: 10699072]
26. Pei L, Zhang Y, Zhang Y, Chu X, Zhang J, Wang R, et al. Peroxisome proliferator-activated receptor gamma promotes neuroprotection by modulating cyclin D1 expression after focal cerebral ischemia. Can J Physiol Pharmacol. 2010; 88:716–723. [PubMed: 20651819]
27. Kapetanovic IM, Horn TL, Johnson WD, Cwik MJ, Detrisac CJ, McCormick DL. Murine oncogenicity and pharmacokinetics studies of 9-cis-UAB30, an RXR agonist, for breast cancer chemoprevention. Int J.Toxicol. 2010; 29:157–164. [PubMed: 20335511]
28. Jayasinghe NR, Cope GH, Jacob S. Morphometric studies on the development and sexual dimorphism of the submandibular gland of the mouse. J Anat. 1990; 172:115–127. [PubMed: 2272897]
29. Díaz-Cruz ES, Furth PA. Deregulated Estrogen Receptor α and p53 Heterozygosity Collaborate in the Development of Mammary Hyperplasia. Cancer Res. 2010; 70:3965–3974. [PubMed: 20466998]
30. Schmittgen TD, Livak KJ. Analyzing real-time PCR data by the comparative CT method. Nat Protocols. 2008; 3:1101–1108.
31. Grubbs CJ, Hill DL, Bland KI, Beenken SW, Lin T-H, Eto I, et al. 9cUAB30, an RXR specific retinoid, and/or tamoxifen in the prevention of methylnitrosourea-induced mammary cancers. Cancer Lett. 2003; 201:17–24. [PubMed: 14580682]
32. Rane SG, Dubus P, Mettus RV, Galbreath EJ, Boden G, Reddy EP, et al. Loss of Cdk4 expression causes insulin-deficient diabetes and Cdk4 activation results in beta-islet cell hyperplasia. Nat Genet. 1999; 22:44–52. [PubMed: 10319860]
33. Malumbres M, Sotillo R, Santamaría D, Galán J, Cerezo A, Ortega S, et al. M. Mammalian cells cycle without the D-type cyclin-dependent kinases Cdk4 and Cdk6. Cell. 2004; 118:493–504. [PubMed: 15315761]
34. Fantl V, Stamp G, Andrews A, Rosewell I, Dickson C. Mice lacking cyclin D1 are small and show defects in eye and mammary gland development. Genes Dev. 1995; 9:2364–2372. [PubMed: 7557388]
35. Sicinski P, Donaher JL, Parker SB, Li T, Fazeli A, Gardner H, et al. Cyclin D1 provides a link between development and oncogenesis in the retina and breast. Cell. 1995; 82:621–630. [PubMed: 7664341]
36. Lapenna S, Giordano A. Cell cycle kinases as therapeutic targets for cancer. Nat Rev Drug Discov. 2009; 8:547–566. [PubMed: 19568282]
37. Malumbres M, Barbacid M. Cell cycle, CDKs and cancer: a changing paradigm. Nat Rev Cancer. 2009; 9:153–166. [PubMed: 19238148]
38. Massagué J. G1 cell-cycle control and cancer. Nature. 2004; 432:298–306. [PubMed: 15549091]
39. Fulda S, Debatin K-M. Sensitization for anticancer drug-induced apoptosis by the chemopreventive agent resveratrol. Oncogene. 2004; 23:6702–6711. [PubMed: 15273734]
40. Millar AW, Lynch KP. Rethinking clinical trials for cytostatic drugs. Nat Rev Cancer. 2003; 3:540–545. [PubMed: 12835674]
41. Paroni G, Fratelli M, Gardini G, Bassano C, Flora M, Zanetti A, et al. Synergistic antitumor activity of lapatinib and retinoids on a novel subtype of breast cancer with coamplification of ERBB2 and RARA. Oncogene. 2011 epub ehead of print.
42. Yang H, Landis-Piwowar K, H Chan T, P Dou Q. Green tea polyphenols as proteasome inhibitors: implication in chemoprevention. Curr Cancer Drug Targets. 2011; 11:296–306. [PubMed: 21247384]

43. Bargonetti J, Reynisdóttir I, Friedman PN, Prives C. Site-specific binding of wild-type p53 to cellular DNA is inhibited by SV40 T antigen and mutant p53. Genes Dev. 1992; 6:1886–1898. [PubMed: 1398068]
44. Whyte P, Williamson NM, Harlow E. Cellular targets for transformation by the adenovirus E1A proteins. Cell. 1989; 56:67–75. [PubMed: 2521301]
45. Henning W, Rohaly G, Kolzau T, Knippschild U, Maacke H, Deppert W. MDM2 is a target of simian virus 40 in cellular transformation and during lytic infection. J Virol. 1997; 71:7609–7618. [PubMed: 9311842]
46. Sladek TL, Laffin J, Lehman JM, Jacobberger JW. A subset of cells expressing SV40 large T antigen contain elevated p53 levels and have an altered cell cycle phenotype. Cell Prolif. 2000; 33:115–125. [PubMed: 10845255]
47. Bocchetta M, Eliasz S, De Marco MA, Rudzinski J, Zhang L, Carbone M. The SV40 large T antigen-p53 complexes bind and activate the insulin-like growth factor-I promoter stimulating cell growth. Cancer Res. 2008; 68:1022–1029. [PubMed: 18281476]
48. Wu L, Goodwin EC, Naeger LK, Vigo E, Galaktionov K, Helin K, et al. E2F-Rb Complexes Assemble and Inhibit cdc25A Transcription in Cervical Carcinoma Cells following Repression of Human Papillomavirus Oncogene Expression. Mol Cell Biol. 2000; 20:7059–7067. [PubMed: 10982822]
49. Liby K, Black CC, Royce DB, Williams CR, Risingsong R, Yore MM, et al. The rexinoid LG100268 and the synthetic triterpenoid CDDO-methyl amide are more potent than Erlotinib for prevention of mouse lung carcinogenesis. Mol Cancer Ther. 2008; 7:1251–1257. [PubMed: 18483313]

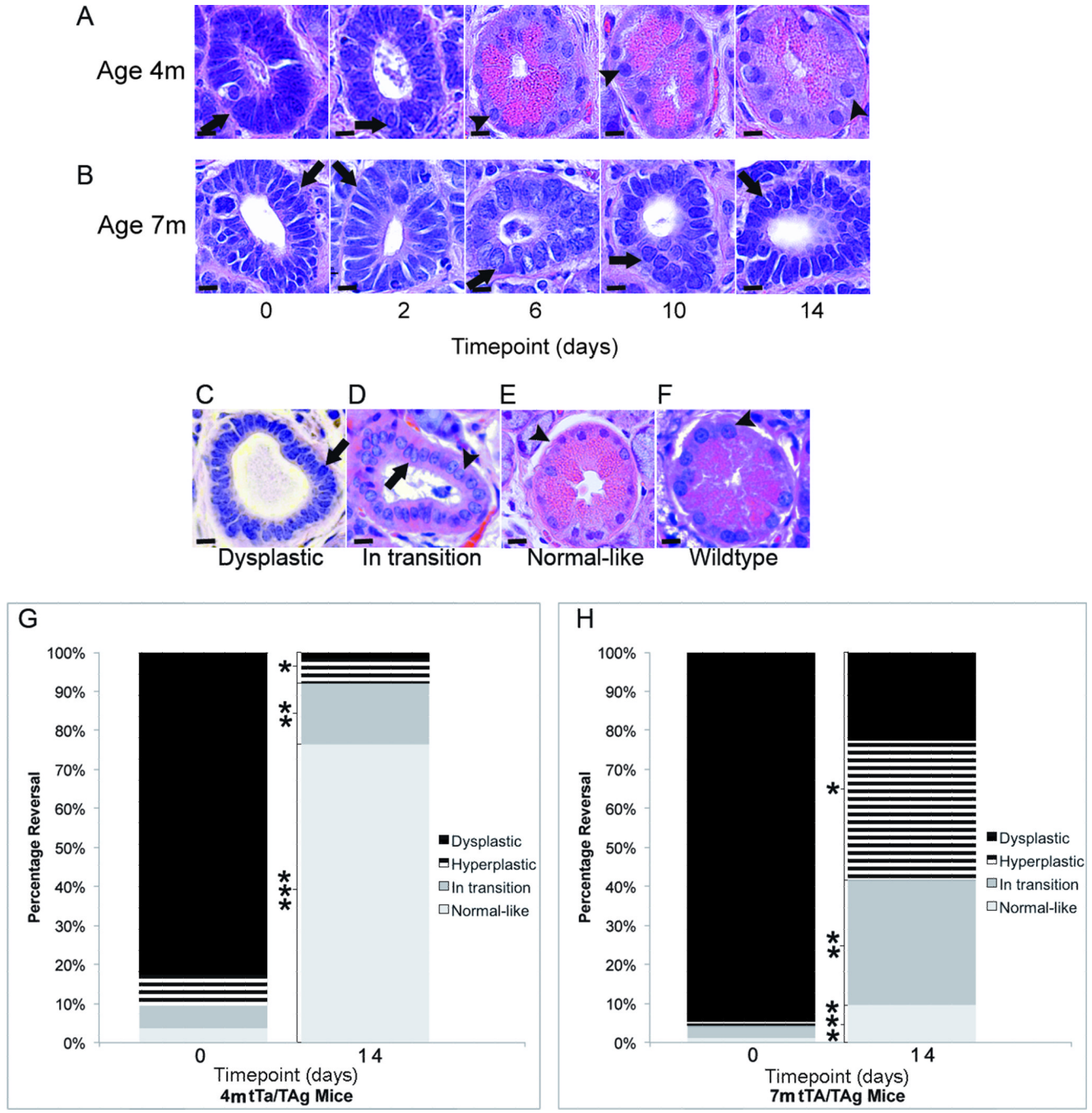

FIGURE 1. Dysplastic and hyperplastic histology was progressively reversed over 14 days when TAg was downregulated at 4- but not 7-months of age

Representative H&E sections illustrate phenotypic reversal of ductal cells in the submandibular salivary gland accompanying TAg downregulation in 4- (A) but not 7- (B) month-old *Tet-op-TAg*$^{MMTV\text{-}tTA}$ (tTa/TAg) mice over a 14-day timecourse. Arrows point to dysplastic ductal epithelial cells with nuclear pleomorphism and hyperchromasia and arrowheads point to striated ductal epithelial cells with normal nuclear appearance. The histological phenotype at both ages consists of varying percentages of hyperplastic and dysplastic (C), in transition (D), and normal-like (E) structures resembling those of wild-type mice (F). Stacked bar graphs shows distribution of hyperplastic and dysplastic, in

transition and normal-like structures before and 14 days after TAg downregulation in 4- (G) and 7-month-old (H) mice. Timepoint (days): 0; prior to TAg downregulation, 2, 6, 10 and 14 indicate the number of days of doxycycline administration to downregulate TAg. m= age in months. Magnification H&E images = 60X. Size bar = 10 μm. *, **, ***:$p<0.05$, Student's *t* test (two-tailed). Cohort sizes at different timepoints: 4m: 0(n = 4), 2(n = 4, 6(n = 4), 10(n = 4), and 14(n=5); 7m: 0(n = 3), 2(n = 3), 6(n = 3), 10(n=3), 14(n = 5).

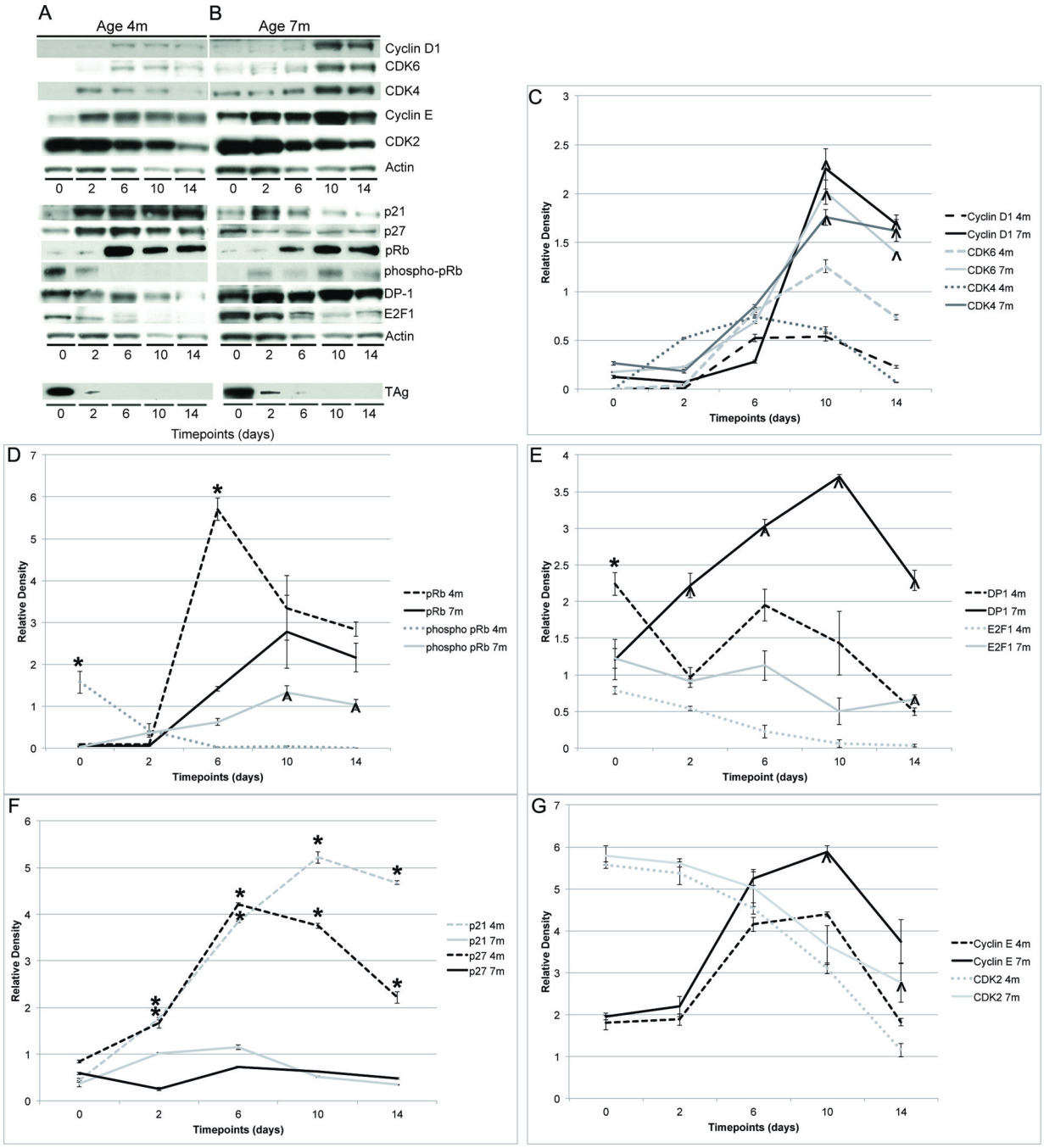

FIGURE 2. Comparison of protein expression patterns when TAg was downregulated in 4- and 7-month-old mice

Representative western blots illustrate the different expression patterns of cell cycle regulatory proteins accompanying TAg downregulation in submandibular salivary tissue in 4- (A) and 7- (B) month-old *Tet-op-TAg*$^{MMTV\text{-}tTA}$ mice over a 14-day timecourse. (C–G) Line graphs illustrate mean relative steady-state protein levels in 4- (dotted lines) and 7- (solid lines) month-old mice before and 2, 4, 6, 10 and 14 days after initiating doxycycline to downregulate TAg. Relative protein expression levels at different timepoints were compared by Student *t* test (two-tailed). (C) Cyclin D1, CDK6 and CDK4 expression levels were significantly higher in 7- as compared to 4-month-old mice at the 10 (Cyclin D1: ^4-

fold ($p<0.02$); CDK6: ^2-fold ($p<0.01$); CDK4: ^3-fold ($p<0.01$) higher) and 14 (Cyclin D1: ^8-fold ($p<0.01$); CDK6: ^4-fold ($p<0.01$); CDK4: ^22-fold ($p< 0.05$) higher) day timepoints. (D) Phosphorylated pRb expression levels were 18-fold lower at the 0 timepoint (*$p<0.05$) and significantly higher at the 10 (^24-fold ($p<0.01$) and 14 (^68-fold ($p<0.018$) day timepoints in 7- as compared to 4-month-old mice. Total pRb levels were 5-fold lower in 7- as compared to 4-month-old mice at the 6-day timepoint (*$p<0.05$). (E) Expression levels of DP-1 were 2-fold lower at the 0 timepoint (*$p<0.005$) and significantly higher at the 2 (^3-fold ($p<0.04$), 6 (^2-fold ($p<0.01$), 10 (^3-fold ($p<0.05$) and 14 (^6-fold ($p<0.01$) day timepoints in 7- as compared to 4-month-old mice. E2F-1 expression was 29-fold higher in the 7- as compared to 4-month-old mice at the 14-day timepoint (^$p<0.05$). (F) Expression levels of p21 and p27 were significantly lower in 7- as compared to 4-month-old mice at the 2 (p21: *2-fold ($p<0.05$), p27: *7-fold ($p<0.03$), 6 (p21: *3-fold ($p<0.01$), p27: *6-fold (*$p<0.05$), 10 (p21: *10-fold ($p<0.04$), p27: 5-fold ($p<0.01$), and 14 (p21: 13-fold ($p<0.01$), p27: 6-fold ($p<0.01$) day timepoints. (G) Expression levels of Cyclin E were ^2-fold higher at 10 days ($p<0.05$) and CDK2 levels were ^2- fold higher at 14 days ($p<0.05$) in 7- as compared to 4-month-old mice. Relative protein expression levels determined by quantification of western blots using densitometry. Mean and SEM indicated for each timepoint. m= age in months. Asterisks (*) indicate statistically significantly lower and carets (^) statistically significantly higher relative expression levels in 7- as compared to 4-month-old mice at the same timepoint (both $p<0.05$, Student's *t* test (two-tailed)., Cohort sizes and timepoints as described (Fig 1).

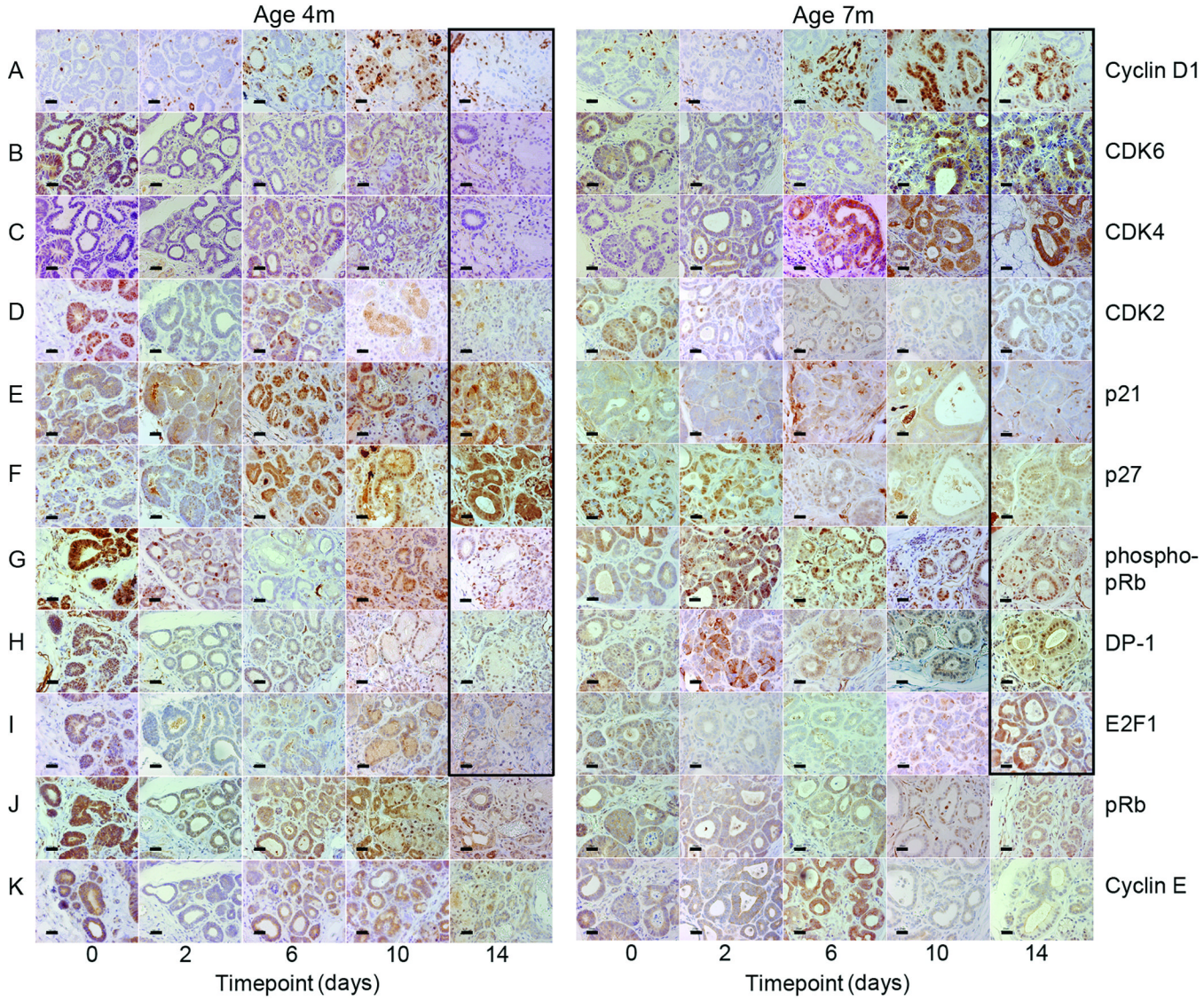

FIGURE 3. Comparison of protein expression patterns in salivary ductal cells when TAg was downregulated in 4- and 7-month-old mice

Representative histological sections of submandibular salivary gland from 4- and 7-month-old *Tet-op-TAg*$^{MMTV\text{-}tTA}$ mice. Immunohistochemical detection of Cyclin D1 (A), CDK6 (B), CDK4 (C), CDK2 (D), pRb (G), DP-1 (H), and E2F-1 (I) was higher and detection of p21 (E) and p27 (F) lower in 7- as compared to 4-month-old mice 14 days after administration of doxycycline to downregulate TAg (panels outlined in black). No differences in expression of total pRb (J) or Cyclin E (K) were found. Digital photographs taken at ×40 and cropped to pre-set dimensions. Size bar = 20 μm. m= age in months. Cohort sizes and timepoints as described (Fig 1).

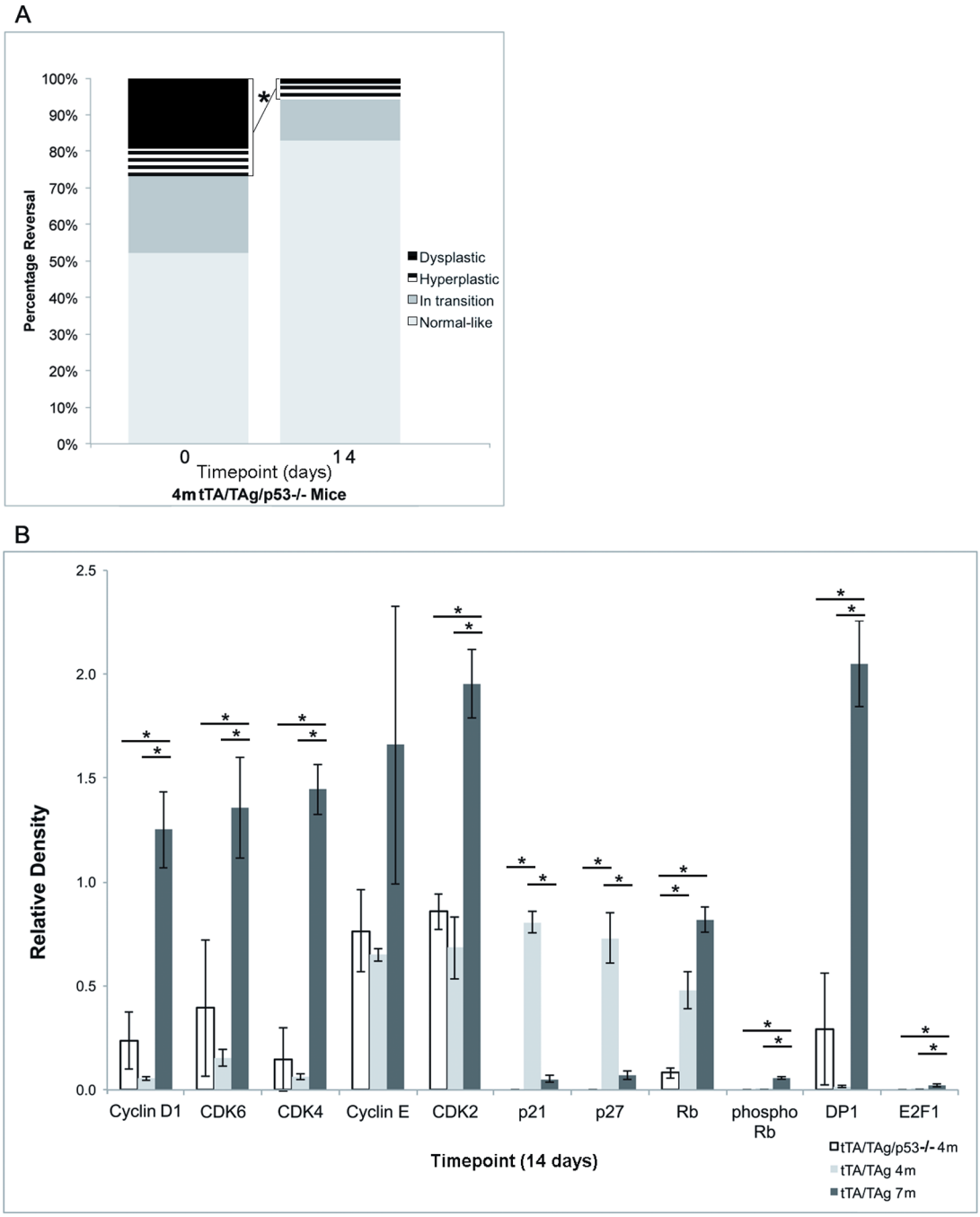

FIGURE 4. p53 was not required for dysplasia reversal in 4-month-old mice

(A) Stacked bar graphs showing distribution of hyperplastic and dysplastic, in transition and normal-like structures before and 14 days after TAg downregulation in submandibular salivary glands of 4-month-old *Tet-op-TAg*$^{MMTV\text{-}tTA/p53-/-}$ (tTa/TAg/p53+/−) mice. (B) Bar graphs comparing relative protein expression levels in submandibular salivary tissue 14 days after TAg downregulation in 4-month-old *Tet-op-TAg*$^{MMTV\text{-}tTA/p53-/-}$ *and Tet-op-TAg*$^{MMTV\text{-}tTA}$ (tTA/TAg) and 7-month-old *Tet-op-TAg*$^{MMTV\text{-}tTA}$ mice. Absence of p53 was associated with significant reductions in relative expression levels of p21 ($p<0.01$), p27 ($p<0.01$) and total pRb ($p<0.05$). No significant differences in expression levels of Cyclin D1, CDK6, CDK4, Cyclin E, CDK2, phosphorylated pRb, DP-1 or E2F-1 were found

between 4-month-old *Tet-op-TAg*$^{MMTV\text{-}tTA/p53^{-/-}}$ *and Tet-op-TAg*$^{MMTV\text{-}tTA}$ mice. There were significant differences in expression of Cyclin D1, CDK6, CDK4, CDK2, pRb, phosphorylated pRb, DP-1 and E2F-1 between 7-month-old *Tet-op-TAg*$^{MMTV\text{-}tTA}$ and 4-month-old *Tet-op-TAg*$^{MMTV\text{-}tTA/p53^{-/-}}$ *and Tet-op-TAg*$^{MMTV\text{-}tTA}$ mice. Relative protein expression levels determined by quantification of western blots using densitometry. Mean and SEM indicated. Timepoints=0 (A) and 14 (A,B) days after administration of doxycycline to downregulate TAg. m= age in months. *:$p<0.05$, Student's *t* test (two-tailed).Cohort sizes by genotype at different timepoints: (A) 4m tTA/TAg/p53−/−: 0(n=5), 14(n=4), (B) 4m tTA/TAg/p53−/− : 14(n=3), 4m tTA/TAg: 14(n=5), 7mtTA/TAg: 14(n=5).

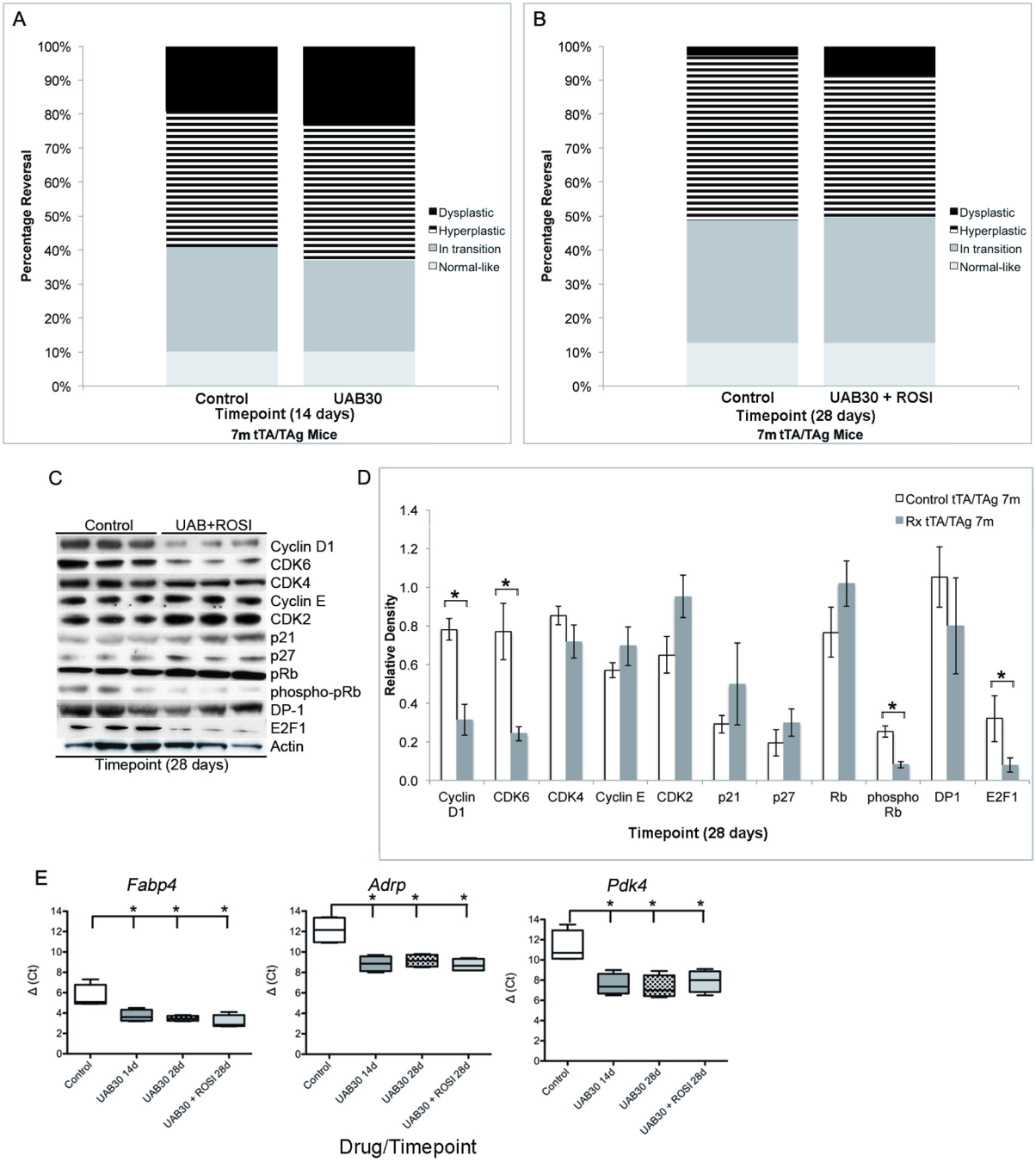

FIGURE 5. Treatment with RXRα and PPARγ ligands UAB30 and rosiglitazone did not change percentage of normal-like structures but did alter expression levels of Cyclin D1, CDK6, phosphorylated Rb and E2F1 in 7-month-old mice

Stacked bar graphs comparing distribution of hyperplastic and dysplastic, in transition and normal-like structures in submandibular salivary glands from untreated control and 14 day-UAB30-treated (A) and in untreated control and 28 day-UAB30+ROSI-treated (B) 7-month-old *Tet-op-TAg*$^{MMTV\text{-}tTA}$- (tTA/TAg) mice in which TAg was coincidentally downregulated by doxycycline. (C) Representative western blots illustrate expression levels of cell cycle regulatory proteins in submandibular salivary tissue of untreated control and 28-day-UAB30+ROSI-treated 7-month-old *Tet-op-TAg*$^{MMTV\text{-}tTA}$ mice that coincidentally

received doxycycline to downregulate TAg. (D) Bar graphs comparing relative protein expression levels in submandibular salivary tissue 28 days after TAg downregulation in control untreated and UAB30+ROSI-treated 7-month-old $TAg^{MMTV\text{-}tTA}$ mice. Expression levels of Cyclin D1 were reduced 2-fold ($p<0.01$), CDK6 were reduced 3-fold ($p<0.02$), phosphorylated pRb were reduced 3-fold ($p<0.05$) and E2F-1 were reduced 4-fold ($p<0.01$) in the UAB30+ROSI-treated mice. Relative protein expression levels determined by quantification of western blots using densitometry. Mean and SEM indicated. (E) Boxplots comparing relative RNA expression levels in submandibular salivary tissue from 7-month-old $TAg^{MMTV\text{-}tTA}$ control untreated mice versus 14-day-UAB30-treated, 28-day-UAB-treated and 28-day-UAB30+ROSI-treated mice with coincident TAg downregulation. Significant increases in expression of *Fabp4, Adrp, Pdk4* were found in all three treatment groups as compared to no treatment controls ($p<0.05$). Timepoints: 14 or 28 days after administration of doxycycline to downregulate TAg. m= age in months.. *:$p<0.05$, Student's *t* test (two-tailed) (D) or Mann Whitney *U* test (E). Cohort sizes by treatment group and timepoint: (A) 7m control 14(n=5), UAB30 14(n=10), (B) 7m control 28(n=5), UAB30+ROSI 28(n=9), UAB30(n=5, data not shown) (C,D) 7m control 28(n=3), UAB30+ROSI 28(n=3), (E) 7m control (n=3), UAB30 14(n=3), UAB30 28(n=3), UAB30+ROSI 28(n=3).

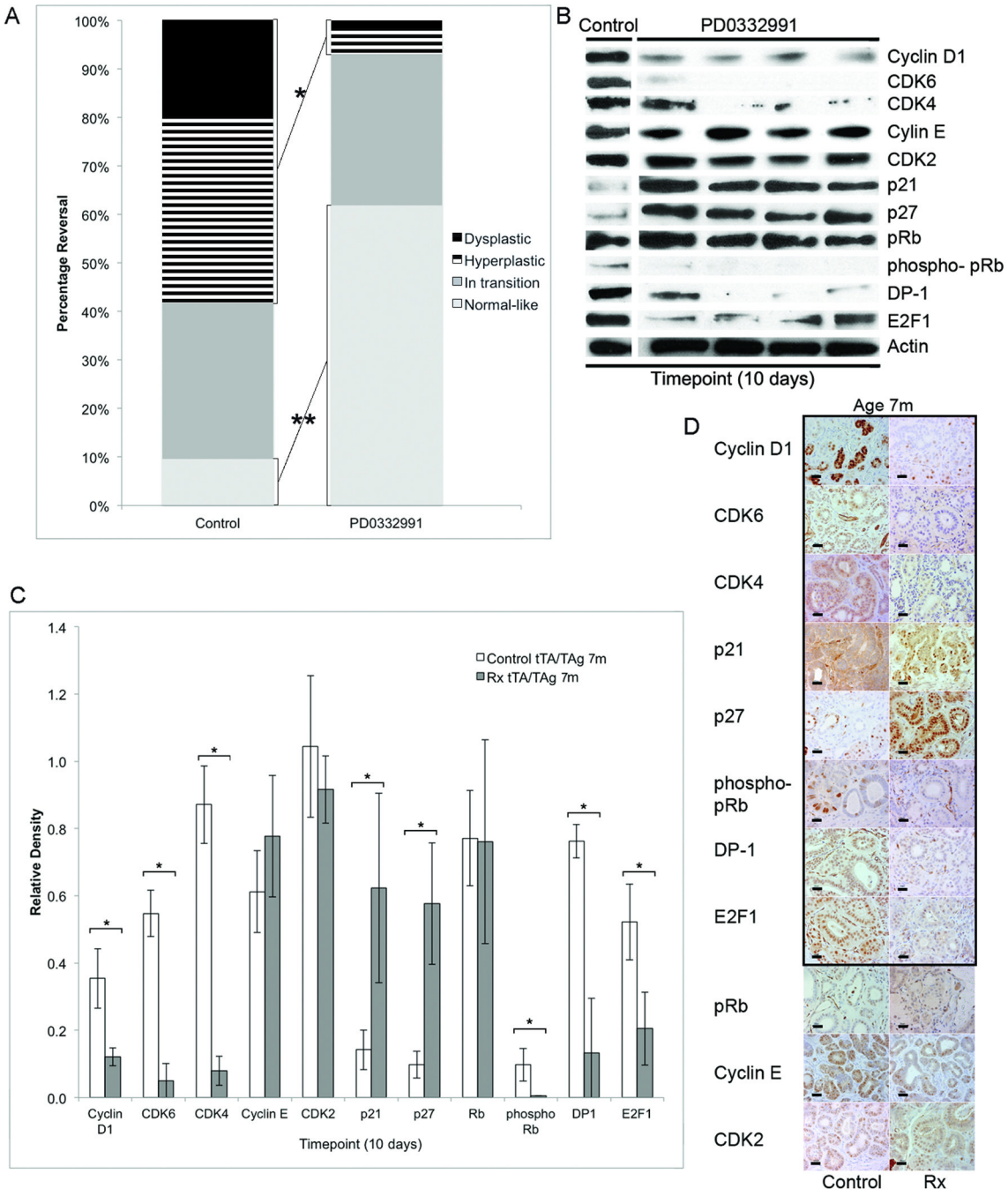

FIGURE 6. CDK4/6 inhibitor, PD0332991, successfully reversed dysplasia in 7-month-old mice

(A) Stacked bar graphs showing distribution of hyperplastic and dysplastic, in transition and normal-like structures in submandibular salivary glands from untreated control and 10-day-PD0332991-treated 7-month-old *Tet-op-TAg*$^{MMTV\text{-}tTA}$ mice in which TAg was coincidentally downregulated by doxycycline. (B) Representative western blots illustrate expression levels of cell cycle regulatory proteins in submandibular salivary tissue in untreated control and 10-day-PD0332991-treated 7-month-old *Tet-op-TAg*$^{MMTV\text{-}tTA}$ mice coincidentally receiving doxycycline to downregulate TAg. Control and PD0332991-treated samples were run on the same blot and cropped to show representative lanes (C) Bar graphs comparing relative expression levels of proteins 10 days after TAg downregulation in

control untreated and PD0332991-treated 7-month-old mice. Expression levels of Cyclin D1 were reduced 3-fold ($p<0.04$), CDK6 were reduced 5-fold ($p<0.003$), CDK4 were reduced 11-fold ($p<0.002$), phosphorylated pRb were reduced 17-fold ($p=0.05$), DP-1 were reduced 6-fold ($p<0.02$), E2F-1 were reduced 2-fold ($p<0.04$), p21 were increased 4-fold ($p<0.05$) and p27 increased 6-fold ($p=0.04$), all significantly changes, in the PD0332991-treated mice as compared to controls. Relative protein expression levels determined by quantification of western blots using densitometry. Mean and SEM indicated. (D) Representative histological sections of submandibular salivary gland from untreated control and PD0332991-treated 7-month-old *Tet-op-TAg*$^{MMTV\text{-}tTA}$ mice illustrated. Immunohistochemical detection of Cyclin D1, CDK6, CDK4, phosphorylated pRb, DP-1, and E2F-1 was lower and detection of p21 (E) and p27 (F) higher in PD0332991-treated as compared to untreated control mice (panels outlined in black). Digital photographs taken at ×40 and all cropped to pre-set dimensions. Size bar = 20 μm. Rx=PD0332991-treated. Timepoint=10 days after downregulation of TAg; m=months. *,**:$p<0.05$, Student's *t* test (two-tailed). Cohort sizes by treatment group and timepoint: 7m control 10(n=3), PD0332991 10(n=4).